nature communications

Article

https://doi.org/10.1038/s41467-025-59783-2

Electroreduction of diluted CO_2 to multicarbon products with high carbon utilization at 800 mA cm^{-2} in strongly acidic media

Received: 24 October 2024

Accepted: 29 April 2025

Published online: 13 May 2025

Check for updates

Xue-Rong Qin[1,2], Jing-Jing Li[1,2], Lin-Lin Wang[1,2], Huan Liu[1], Zuo-Tao Yang[1], Guo-Jin Feng[1], Xiao-Ran Wang[1], Xuan-Xuan Cheng[1], Chao Zhang[1], Zi-You Yu[1] ✉ & Tong-Bu Lu[1] ✉

Acidic CO_2 electroreduction using diluted CO_2 (as in flue gas) as the feedstock can simultaneously circumvent the CO_2 purification step and lower the carbon loss in conventional alkaline or neutral electrolyte, and thus is highly desired but has rarely been achieved thus far. Herein, we report a simple and general strategy using an imidazolium-based anion-exchange ionomer as the coating layer, which could enrich the diluted CO_2 to generate a high local CO_2 concentration, and simultaneously block the proton transport to the cathode surface to suppress the competing hydrogen evolution reaction. As a result, the ionomer-modified Cu catalyst can achieve an efficient electroreduction of diluted CO_2 (15 vol% CO_2) to multicarbon (C_{2+}) products in strong acid (pH 0.8), with a high C_{2+} Faradaic efficiency of 70.5% and a high single-pass carbon efficiency of 73.6% at a current density of 800 mA cm^{-2}, competitive with that obtained with pure CO_2. These findings provide opportunity for the direct electrochemical conversion of flue gas into valuable products with high efficiency.

Electrocatalytic carbon dioxide reduction (CO_2R) is a sustainable way to convert CO_2 into value-added chemicals and fuels by using renewable electricity, contributing to the development of a carbon-neutral economy[1–6]. Currently, most of the related studies have been focused on the use of high-purity CO_2 gas (> 99%) as the feedstock for electrocatalytic CO_2R, whereas industrial flue gas as the primary form of CO_2 emission, contains low-concentration CO_2 gas (~15 vol %)[7–10]. This means that we need to capture and enrich the diluted CO_2 to generate high-purity CO_2 for subsequent CO_2R electrolysis[10]. However, CO_2 purification from flue gas is an energy-intensive process and usually costs $70–100 per ton of CO_2[8,11–13]. It would be very promising to directly utilize the diluted CO_2 streams as the feedstock for the cost-effective CO_2 electroreduction into valuable products[7–10]. Unfortunately, when diluted CO_2 gas is used as the feedstock, the competing hydrogen evolution reaction (HER) usually becomes the dominated reaction owing to the low CO_2 concentration, thus resulting in the unsatisfactory CO_2R performance[7,10,14]. To date, the direct electroreduction of diluted CO_2 into valuable products with high selectivity still remains a formidable challenge.

Among the diverse CO_2R products, multicarbon (C_{2+}) products, including ethylene, ethanol, and acetate, have received broad attention for their high market price and energy density[3,15–18]. Up to now, most reported catalysts and reactors for CO_2R-to-C_{2+} conversion mainly operate in alkaline or neutral electrolytes, in which the local

[1]MOE International Joint Laboratory of Materials Microstructure, Institute for New Energy Materials and Low Carbon Technologies, School of Materials Science & Engineering, Tianjin University of Technology, Tianjin, China. [2]These authors contributed equally: Xue-Rong Qin, Jing-Jing Li, Lin-Lin Wang.
✉e-mail: yuziyou@email.tjut.edu.cn; lutongbu@tjut.edu.cn

alkaline microenvironment can help to activate CO_2 molecules and facilitate the C–C coupling step while suppress the HER[18–21]. However, the input CO_2 suffers from serious consumption by reacting with hydroxide ions to form unnecessary carbonate or bicarbonate ions, leading to a very low single-pass carbon efficiency (SPCE, typically ≤ 25%) for C_{2+} products[22,23]. The further regeneration of lost CO_2 from (bi)carbonate requires an additional ~ 50% of input energy[22]. Using acidic electrolytes provides an alternative route to alleviate the (bi) carbonate formation and carbon loss problem, but the fast reaction rate for kinetically favorable HER usually leads to a low CO_2R Faradaic efficiency (FE) in this condition[24–27]. Recently, enormous efforts and attempts have been devoted to exploring diverse strategies to suppress the HER kinetics for effective CO_2R-to-C_{2+} conversion in acid[21,22,28–33]. However, high-purity CO_2 was still used as the fed gas to improve the selectivity for electrocatalytic CO_2R. The direct utilization of diluted CO_2 (as in flue gas) instead of pure CO_2 to generate C_{2+} products with high FE in strong acid is highly desired but has never been achieved.

For a bare Cu catalyst under the diluted CO_2 condition, its low local CO_2 concentration would lead to the easy occurrence of the kinetically favored HER over CO_2R (Fig. 1a). We postulate that a catalyst containing a proper CO_2 enriching layer can concentrate the diluted CO_2 to generate a high local CO_2 concentration at the catalyst surface. We thus engineered Cu surface with an imidazolium-based anion-exchange ionomer coating layer, which can capture and enrich diluted CO_2 to obtain a high local CO_2 concentration, and simultaneously obstruct the proton transport to suppress HER, thereby forming rich gas–liquid–solid three-phase interfaces for efficient electroreduction of diluted CO_2 in acidic media (Fig. 1a). With diluted CO_2 (15 vol% CO_2) as the feedstock and strongly acidic solution (pH 0.8) as the electrolyte, our catalyst achieved a high C_{2+} FE of 70.5% and a high SPCE of 73.6% at a current density of 800 mA cm^{-2}, surpassing the reported CO_2R-to-C_{2+} performance achieved in pure CO_2 atmosphere.

Results

CO_2 capture and transport

We selected Sustainion ionomer (Fig. 1a), a commercially available imidazolium-based anion-exchange ionomer, to enrich the local CO_2 concentration and increase the CO_2-to-water ratio, on account of the strong CO_2 affinity with imidazolium group[34–37]. A flat glassy carbon electrode (GCE) was used as the substrate for the observation of the CO_2 adsorption behavior of Sustainion ionomer. Sustainion circular micropatterns with diameters of ~300 μm were deposited on GCE (denoted as GCE@Sustainion) through a shadow mask-assisted

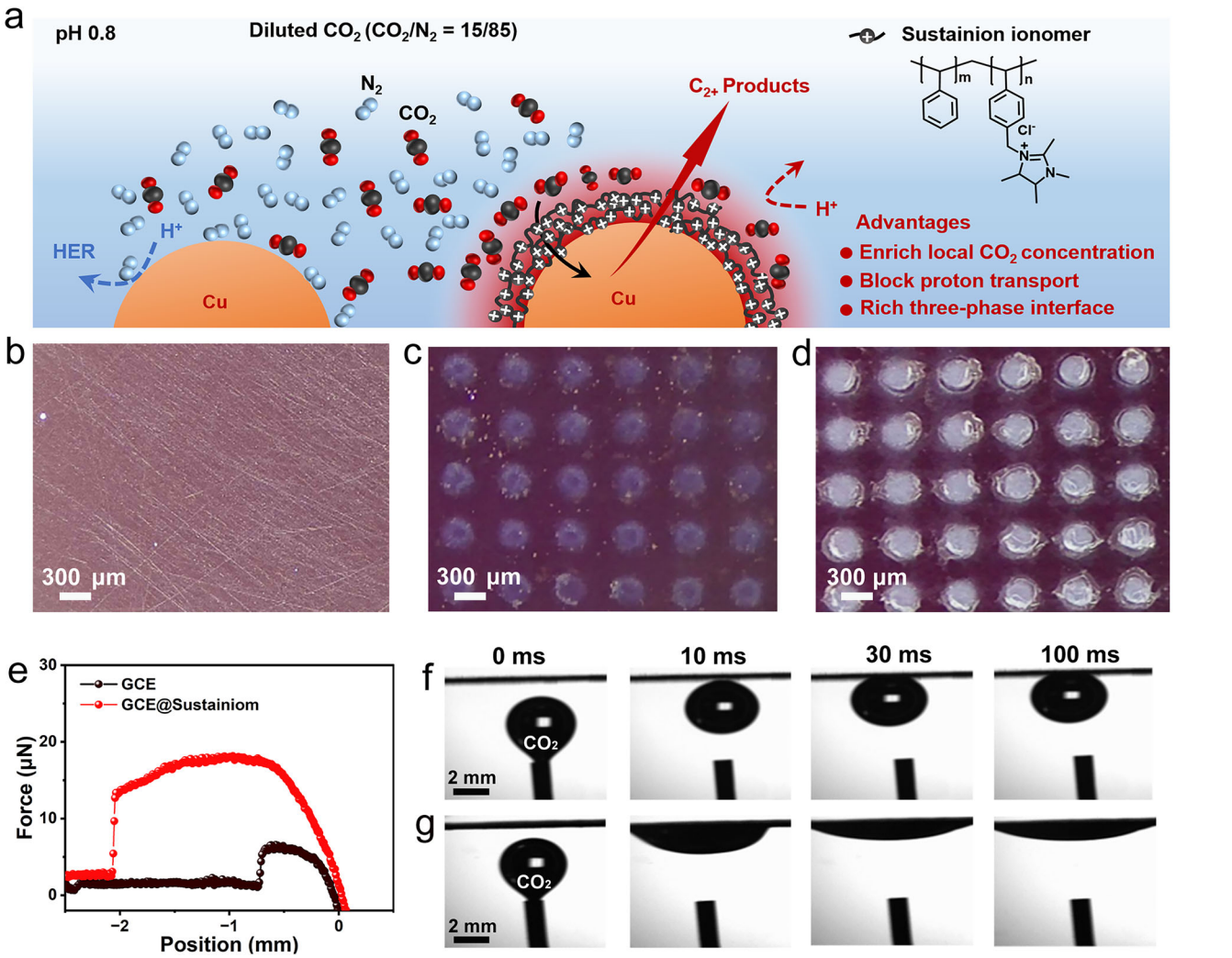

Fig. 1 | CO_2 capture and transport. a Schematic illustration of the catalyst with altered microenvironment after coating Sustainion layer for efficient electroreduction of diluted CO_2 in strong acid. **b** Digital photograph for bare glassy carbon electrode (GCE) in pure water after bubbling CO_2 gas. **c**, **d** Digital photographs for GCE@Sustainion in pure water before (**c**) and after (**d**) bubbling CO_2 gas. **e** CO_2 gas bubble adhesive force measurements for GCE and GCE@Sustainion. **f**, **g** Real-time CO_2 bubble transport behaviors for GCE (**f**) and GCE@Sustainion (**g**).

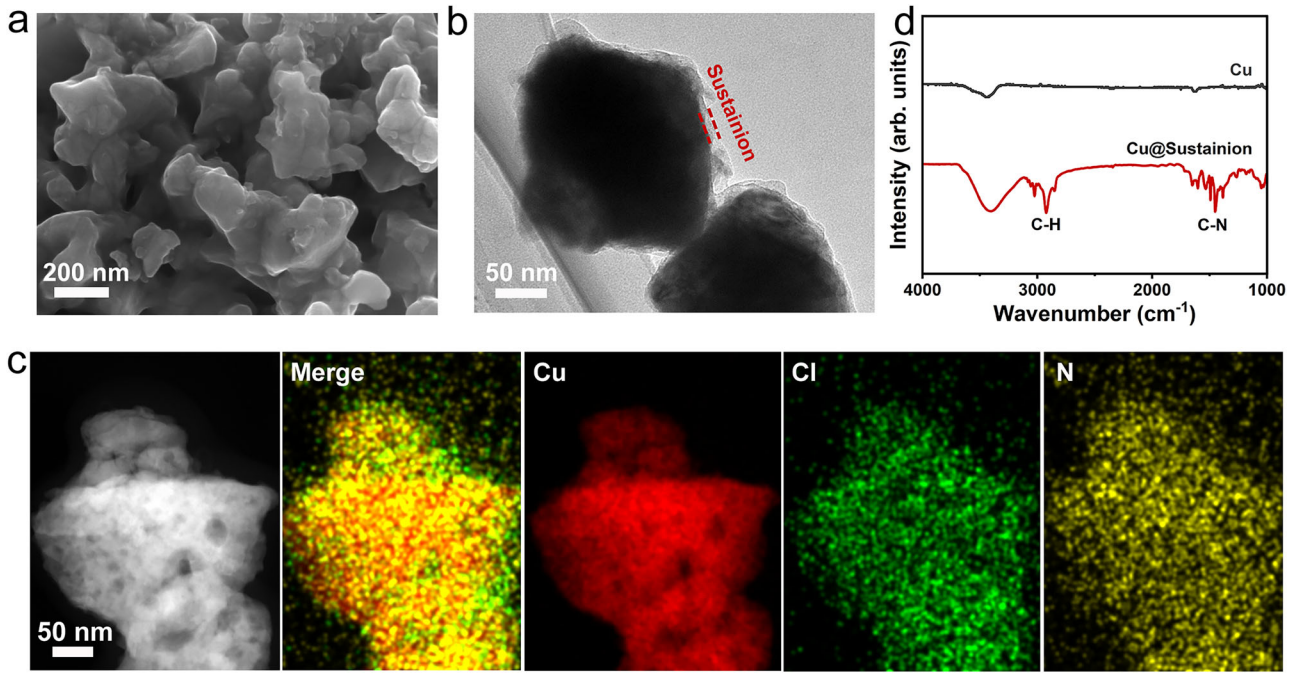

Fig. 2 | Synthesis and characterization of Cu@Sustainion catalyst. a–c SEM image (**a**), TEM image (**b**), and EDX elemental mappings (**c**) of Cu@Sustainion catalyst. **d** FTIR spectra of Cu and Cu@Sustainion catalysts.

method (see the Methods section for details, Supplementary Fig. 1). By continuously bubbling CO_2 gas onto the electrode surface, we found that no CO_2 bubbles could be observed on the bare GCE surface (Fig. 1b and Supplementary Fig. 2), but a large number of CO_2 bubbles were captured by the Sustainion micropatterns on GCE@Sustainion (Fig. 1c, d). This indicates the strong affinity of Sustainion ionomer to CO_2, which was further confirmed via the bubble adhesive force measurements. The GCE@Sustainion electrode has a CO_2 adhesive force of 18.2 μN, ~3 times higher than that for bare GCE (Fig. 1e). We also performed the real-time bubble adhesion experiments to monitor the dynamic CO_2 transport on the electrode surface using a high-speed camera. The CO_2 bubbles exhibited a steadily pinning state on the GCE surface for up to 100 ms (Fig. 1f), whereas the bubbles quickly spread on the Sustainion ionomer surface in solution within 30 ms (Fig. 1g), indicative of the rapid CO_2 transport on the surface of Sustainion ionomer with a superaerophilic feature. In addition, water contact angle tests showed that the contact angle value increases sharply from 54° for GCE to 122° for GCE@Sustainion (Supplementary Fig. 3), revealing the hydrophobicity of the Sustainion surface, which would help to block the proton transport from the bulk solution to the catalyst surface in acidic electrolyte. The above observations demonstrate that the Sustainion coating layer can effectively facilitate CO_2 capture and transport, and simultaneously restrict the proton transport to catalyst surface, thereby promoting the formation of stable and rich gas–liquid–solid three-phase interfaces for electrocatalytic CO_2R (Fig. 1a).

Synthesis and characterization of catalysts

We further coated the Sustainion ionomer on the surface of Cu catalyst for the study of electrocatalytic CO_2R. We first synthesized a Cu-based metal-organic framework (Cu-BTC) as the Cu precursor by mixing copper nitrate and benzene-1,3,5-tricarboxylate (BTC) in methanol solution at room temperature (Supplementary Fig. 4). Then CuO nanoparticles were obtained through annealing the Cu-BTC in air at 350 °C (Supplementary Fig. 5). Subsequently, CuO nanoparticles and Sustainion ionomer were mixed under ultrasonication and sprayed onto a carbon paper-based gas-diffusion electrode (GDE), which were further subjected to an electrochemical reduction process to form the Cu@Sustainion electrode with the loading amounts of 1.4 mg cm^{-2} for Cu and 0.1 mg cm^{-2} for Sustainion ionomer (see the Methods section for details).

Scanning electron microscopy (SEM) and transmission electron microscopy (TEM) images (Supplementary Fig. 6) show that bare Cu has a smooth nanoparticle morphology with diameters of 150–200 nm. After coating of Sustainion ionomer, Cu@Sustainion catalyst exhibits a rough surface with an ionomer layer thickness of 10–30 nm (Fig. 2a, b and Supplementary Fig. 7). X-ray diffraction (XRD) patterns (Supplementary Fig. 8) show that Cu and Cu@Sustainion catalysts have the same diffraction peaks from the cubic Cu phase (JCPDS no. 04-0836). Energy-dispersive X-ray (EDX) elemental mappings (Fig. 2c) revealed that Cl and N elements were uniformly distributed on the Cu surface, further confirming the coating of the Sustainion ionomer layer on the surface of Cu nanoparticles.

The Fourier transform infrared (FTIR) spectrum of Cu@Sustainion (Fig. 2d) shows the absorption bands characteristic of Sustainion ionomer, consistent with the previous report[38]. From the X-ray photoelectron spectra (XPS) and Auger spectra of Cu element (Supplementary Fig. 9), we can see that bare Cu and Cu@Sustainion catalysts have the same Cu valence states with primary Cu^0 and minor Cu^+ species, indicative of the unaffected Cu valence states after the coating of Sustainion ionomer. In addition, the prominent Cl 2*p* and N 1*s* XPS signals from Sustainion ionomer were observed on the Cu@Sustainion catalyst (Supplementary Fig. 9). The CO_2 transport and water contact angle measurements (Supplementary Figs. 10 and 11) revealed that Cu@Sustainion exhibits similar aerophilic and hydrophobic behavior to the above GCE@Sustainion (Fig. 1f, g and Supplementary Fig. 3), indicating the unaltered surface feature of Sustainion ionomer.

Electrocatalytic CO_2R performance in pure CO_2

To verify the predicted enhancement role of the Sustainion coating layer, we first evaluated the electrocatalytic CO_2R performance for Cu@Sustainion and Cu catalysts in a flow cell with pure CO_2 gas fed at the GDE backside (Fig. 3a). A strongly acidic solution containing 3.0 M KCl with 0.05 M H_2SO_4 (pH 0.8) was used as the catholyte[21,22,33].

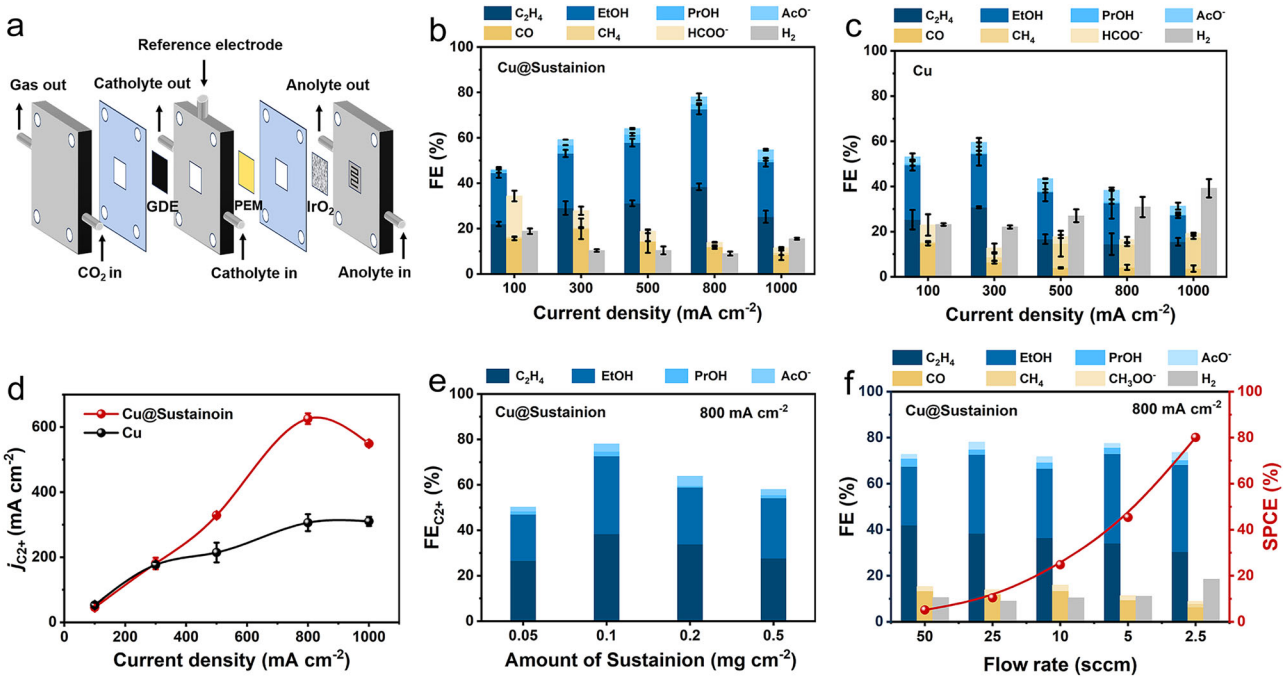

Fig. 3 | Electrocatalytic CO_2R performance in pure CO_2. **a** Schematic illustration of the configuration of a flow cell. Electrolyte: 3.0 M KCl with 0.05 M H_2SO_4 solution (pH 0.8). CO_2 flow rate (pure CO_2): 25 sccm. **b**, **c** FEs of all products on Cu@Sustainion (**b**) and Cu (**c**) at different current densities. **d** C_{2+} partial current densities on Cu@Sustainion and Cu. **e** FEs of C_{2+} products on Cu@Sustainion with different Sustainion loading amounts at 800 mA cm^{-2}. **f** FEs of all products and SPCEs on Cu@Sustainion with different CO_2 flow rates at 800 mA cm^{-2}. The error bars represent the standard deviation of three independent measurements.

The solution-phase and gas-phase products were quantified via nuclear magnetic resonance (NMR) spectroscopy and online gas chromatography, respectively. The CO_2R product distribution for Cu@Sustainion catalyst (Fig. 3b) shows the increased C_{2+} FE within the current density range from 100 to 800 mA cm^{-2}. A maximum C_{2+} FE of 78.2 ± 2% with a C_{2+} partial current density of 625.6 ± 16 mA cm^{-2} was achieved at 800 mA cm^{-2}, and the FE for HER was substantially suppressed to below 10%. In contrast, the Cu catalyst displayed a gradual decrease of C_{2+} FE and a gradual increase of HER at current densities of > 300 mA cm^{-2} (Fig. 3c). The C_{2+} partial current density for Cu catalyst was merely 305.6 ± 24 mA cm^{-2} at a total current density of 800 mA cm^{-2}, with a C_{2+} FE of 38.2 ± 3% and a H_2 FE of 30.9 ± 4%. Therefore, Cu@Sustainion catalyst exhibits a remarkably enhanced C_{2+} partial current density at high current densities (Fig. 3d). It should be noted that the similar CO_2R activity for Cu and Cu@Sustainion at 100-300 mA cm^{-2} could be attributed to the slow consumption and enough supply of CO_2 gas at these low current densities.

We then measured the electrochemically active surface area (ECSA) for Cu@Sustainion and Cu catalysts (Supplementary Fig. 12). Cu@Sustainion catalyst has a smaller ECSA value than Cu catalyst, implying that the enhancement in CO_2R activity for Cu@Sustainion originates from the intrinsic activity rather than the ECSA. We also optimized the loading amount of Sustainion ionomer and found that Cu@Sustainion with a Sustainion loading of 0.1 mg cm^{-2} exhibited the highest C_{2+} FE (Fig. 3e and Supplementary Fig. 13). The electrocatalytic CO_2R operated in strongly acidic electrolytes can alleviate the (bi) carbonate formation, thus circumventing the CO_2 utilization limitation typically for alkaline and neutral media[22,26,27]. When the CO_2 flow rate decreased from 50 to 2.5 standard cubic centimeters per minute (sccm), Cu@Sustainion catalyst still retained a high C_{2+} FE of ~75%. Therefore, a SPCE of 80.1% for all CO_2R products (~ 61% for C_{2+} products) was achieved at 2.5 sccm and 800 mA cm^{-2} (Fig. 3f). Such a SPCE is clearly competitive with those reported in acidic, alkaline, and neutral electrolytes (Supplementary Table 1).

We further evaluated the CO_2R stability for Cu@Sustainion catalyst at a constant current density of 500 mA cm^{-2} (Supplementary Fig. 14). The Cu@Sustainion catalyst could retain a high C_{2+} FE of 65–70% for 16 h continuous operation at 500 mA cm^{-2}. Postmortem characterizations revealed the unchanged morphology and structure for Cu@Sustainion after CO_2 electrolysis (Supplementary Figs. 15 and 16). The above prominent CO_2R activity and stability for Cu@Sustainion could be attributed to the unique Sustainion coating layer, which helps to form stable and rich three-phase interfaces to promote the CO_2R conversion and simultaneously suppress the HER in strong acid.

Moreover, we found that our ionomer coating strategy is quite general. When the Cu component in Cu@Sustainion was replaced by other Cu catalysts, such as commercial Cu nanoparticles (Com-Cu) and electrodeposited Cu microcrystals (ED-Cu), the resulting Sustainion-coated catalysts, denoted as Com-Cu@Sustainion and ED-Cu@Sustainion, respectively, exhibited much improved CO_2R-to-C_{2+} activity and significantly inhibited HER with respect to the uncoated Cu counterparts (Supplementary Figs. 17–20). For example, ED-Cu@Sustainion gives a maximum C_{2+} FE of 76.5% at 800 mA cm^{-2}, much higher than that for ED-Cu (mere 35.7%) at the same current density (Supplementary Fig. 20).

CO_2R enhancement mechanism

We further conducted multiple characterizations to uncover the origin of the enhanced electrocatalytic CO_2R performance after ionomer coating. The CO_2 concentration at the catalyst surface was determined via an electrochemical method using 1,4-benzoquinone as a redox probe, which can reversibly bind with CO_2 molecules[39–42]. As the local CO_2 concentration can shift the redox potential of 1,4-benzoquinone (Fig. 4a, b), the potential difference (ΔE) in CO_2 and Ar atmospheres for different electrode surfaces can reflect the different local CO_2 concentrations. Cu@Sustainion has a ΔE value of 110 mV, larger than that for Cu catalyst (85 mV), suggesting that the local CO_2 concentration at

https://doi.org/10.1038/s41467-025-59783-2

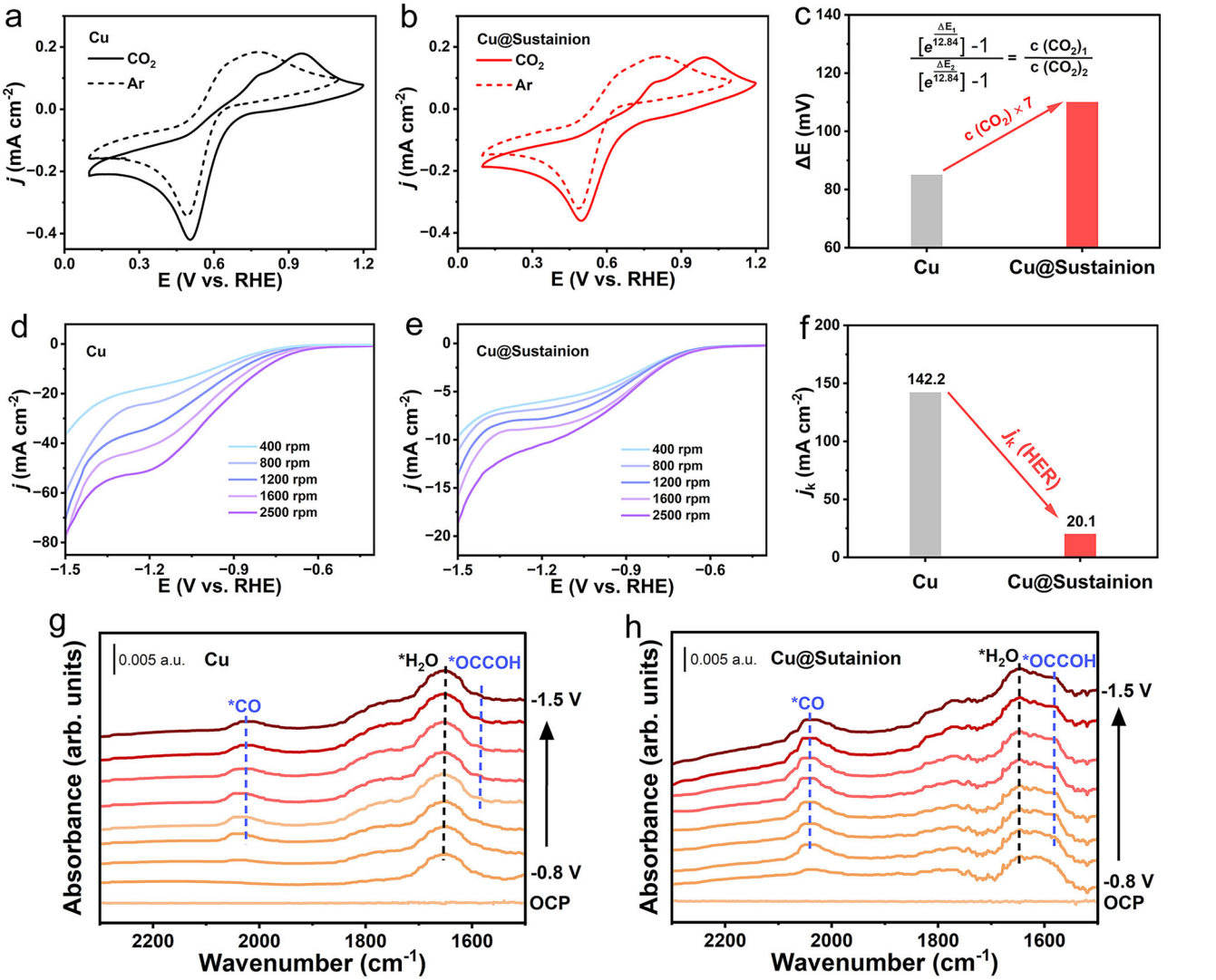

Fig. 4 | Mechanistic investigations. a, **b** Cyclic voltammetry curves of 1 mM 1,4-benzoquinone for Cu (**a**) and Cu@Sustainion (**b**) in Ar-saturated and CO_2-saturated 0.1 M $NaHCO_3$ solution. **c** The potential difference (ΔE) in CO_2 and Ar atmospheres and the derived local CO_2 concentration for Cu and Cu@Sustainion. **d**, **e** Linear sweep voltammetry curves with iR correction for Cu (**d**) and Cu@Sustainion (**e**) at different electrode rotating speeds in Ar-saturated 3 M KCl with 0.05 M H_2SO_4. **f** HER kinetic current density (j_k) for Cu and Cu@Sustainion. **g**, **h** In situ ATR-SEIRAS spectra for Cu (**g**) and Cu@Sustainion (**h**) at different applied potentials.

the catalyst surface increased by ~7 times after Sustainion coating (Fig. 4c and Supplementary Table 2 for details). CO_2 gas adsorption measurements reveal that Cu@Sustainion with 6.7 wt% Sustainion displays a CO_2 adsorption capacity 1.7 times higher than Cu (Supplementary Fig. 21), indicating the effective enrichment of CO_2 concentration on the Cu@Sustainion surface.

To verify whether the enhanced CO_2R activity merely originates from the CO_2 enrichment on the hydrophobic chain of Sustainion ionomer, we prepared two control samples by coating the hydrophobic Nafion and polytetrafluoroethylene (PTFE) on Cu surfaces (Supplementary Fig. 22). They could moderately improve the CO_2R activity of Cu, but their activities are still much lower than that for Cu@Sustainion (Supplementary Fig. 23). We further conducted cyclic voltammetry tests and in-situ Raman spectra in organic electrolyte to investigate the role of imidazolium cation (Supplementary Figs. 24 and 25), indicating the strong interaction between electrochemically-generated imidazolium radical and CO_2 molecule. There observations suggest that the hydrophobic chain of Sustainion can enrich CO_2 gas, and the imidazolium cation can chemically interact with CO_2 to enhance the binding ability, which together result in the increased CO_2 adsorption and enrichment near the Cu catalyst surface.

To investigate the effect of Sustainion ionomer on proton diffusion, we conducted rotating disk electrode (RDE) experiments for Cu and Cu@Sustainion in Ar-saturated 3 M KCl with 0.05 M H_2SO_4, where HER is the exclusive reaction. The polarization curves for both electrodes exhibited a current density plateau between −1.1 V and −1.4 V, as a result of the HER from diffusion-limiting hydronium reduction (Supplementary Fig. 26)[32,43,44]. Compared with Cu, Cu@Sustainion showed smaller plateau current densities at all tested electrode rotating speeds (Fig. 4d, e), indicative of the low local proton concentration with restricted mass transport to the electrode surface. For example, at an electrode rotating speed of 2500 rotations per min (rpm), Cu@Sustainion gave a diffusion-limiting HER plateau current density of ~11 mA cm^{-2}, much lower than that for Cu catalyst (~55 mA cm^{-2}). According to the linear fitting of the Koutecky–Levich equation (Supplementary Fig. 27), we could determine the HER kinetic current density (j_k) decreased from 142.2 to 20.1 mA cm^{-2} after Sustainion coating (Fig. 4f), indicating that the Sustainion layer could obstruct the proton diffusion to substantially suppress HER. The

https://doi.org/10.1038/s41467-025-59783-2

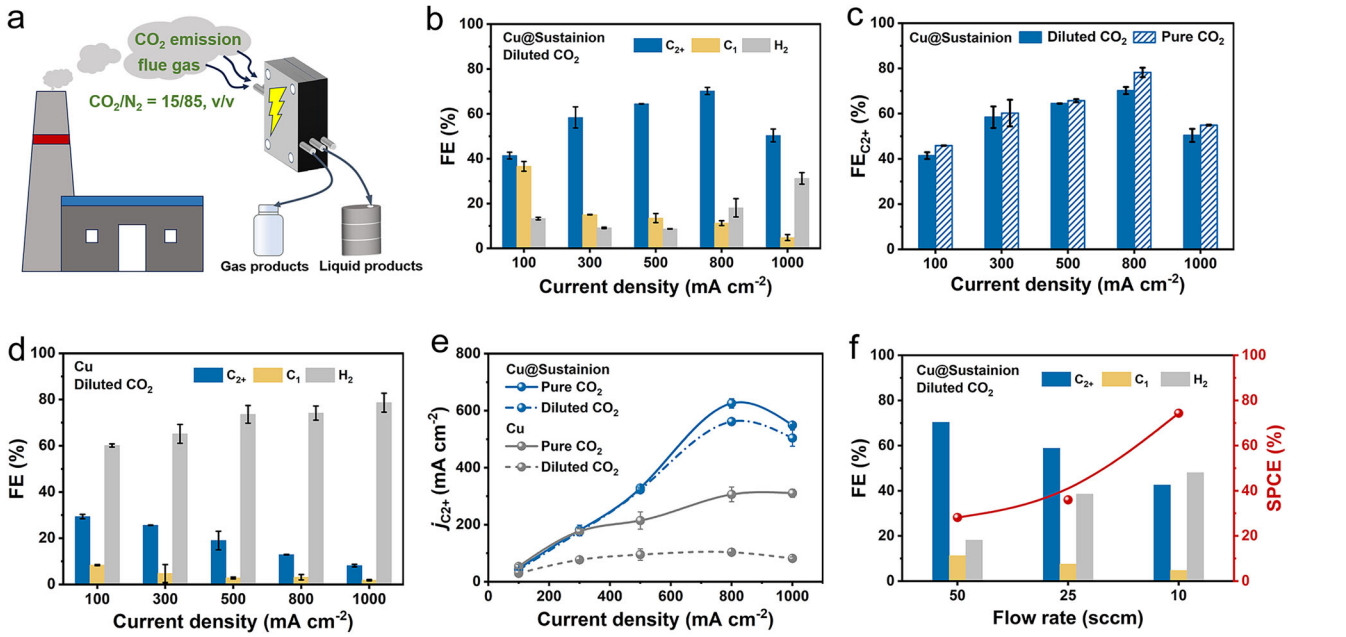

Fig. 5 | Electrocatalytic CO_2R performance in diluted CO_2. **a** Schematic illustration of the conversion of diluted CO_2 into fuels via CO_2 electrolysis. Electrolyte: 3.0 M KCl with 0.05 M H_2SO_4 solution (pH 0.8). Total gas (CO_2/N_2 = 15/85) flow rate: 50 sccm. **b** FEs of all products on Cu@Sustainion in diluted CO_2. **c** FEs of C_{2+} products on Cu@Sustainion in diluted and pure CO_2. **d** FEs of all products on Cu in diluted CO_2. **e** Partial current densities of C_{2+} on Cu@Sustainion and Cu in diluted and pure CO_2. **f** FEs and SPCEs on Cu@Sustainion with different flow rates at 800 mA cm^{-2} in diluted CO_2. The flow rate is the total gas flow rate containing CO_2 and N_2 with 15% CO_2. The error bars represent the standard deviation of three independent measurements.

ECSA-normalized polarization curves and kinetic current densities further confirmed this observation (Supplementary Fig. 28).

We further performed in-situ attenuated total reflection surface-enhanced infrared absorption spectroscopy (ATR-SEIRAS) to monitor the change of reaction intermediates at different applied voltages during acidic CO_2R (Supplementary Fig. 29). As shown in Fig. 4g, h, the distinct bands at ~2030 cm^{-1} assigned to *CO intermediates[45–47], were observed on both Cu and Cu@Sustainion catalysts. The band intensity for Cu@Sustainion is significantly stronger than that for Cu, indicative of the efficient activation and reduction of the CO_2 molecule to *CO intermediate after Sustainion coating. In addition, the bands at around 1585 cm^{-1} were ascribed to the C = O stretching band of *OCCOH intermediates formed via C–C coupling[45,48,49]. Compared with Cu catalyst with a weak C = O band started at −1.1 V, Cu@Sustainion favorably formed this band at a more positive potential and exhibited a stronger band intensity, suggesting that the Sustainion-coated catalyst could readily facilitate the CO dimerization process for the promoted CO_2-to-C_{2+} conversion in acidic electrolyte.

Electrocatalytic CO_2R performance in diluted CO_2

To demonstrate the potential of the direct conversion of flue gas into fuels via CO_2 electrolysis (Fig. 5a), we conducted electrocatalytic CO_2R tests using a simulated flue gas with 15 vol % CO_2 (CO_2/N_2 = 15/85, v/v) as the feed stream at pH 0.8. It is interesting to note that the product FEs for Cu@Sustainion catalyst in diluted CO_2 is close to those in pure CO_2 (Fig. 5b, c and Supplementary Fig. 30). Impressively, Cu@Sustainion can still give a very high C_{2+} FE of 70.5 ± 1.6% at 800 mA cm^{-2} in diluted CO_2, only slightly lower than that of 78.2 ± 2% in pure CO_2, thereby retaining 90% of C_{2+} partial current density at 800 mA cm^{-2} (Fig. 5e). In stark contrast, when the feed gas was switched from pure CO_2 to diluted CO_2, the C_{2+} partial current density at 800 mA cm^{-2} for Cu catalyst decreased markedly from 305.6 ± 24 to 104.2 ± 1 mA cm^{-2} with only 34% retention (Fig. 5d, e and Supplementary Fig. 31). Moreover, the SPCE tests revealed that Cu@Sustainion can achieve a high SPCE of 73.6% at a total gas flow rate of 10 sccm containing 15% CO_2 (Fig. 5f), which is comparable to reported benchmark results under pure CO_2 conditions (Supplementary Table 1). These results indicate that Cu@Sustainion could substantially retain the CO_2R performance in diluted CO_2, which can be attributed to the effective enrichment of the diluted CO_2 by the Sustainion layer to generate a high local CO_2 concentration at the catalyst surface, thereby leading to the remarkable CO_2R performance in low-concentration CO_2.

Discussion

In summary, we report an imidazolium-based anion-exchange ionomer-coated Cu catalyst, which can achieve a high C_{2+} FE of 70.5% and a high SPCE of 73.6% at a current density of 800 mA cm^{-2} when fed with diluted CO_2 (15 vol% CO_2) at pH 0.8. The CO_2R performance using diluted CO_2 as the feedstock is competitive with results in a pure CO_2 atmosphere. Such good performance could be attributed to the ionomer coating layer that can significantly enrich the diluted CO_2 to generate a high local CO_2 concentration at the catalyst surface, and greatly suppress the HER by obstructing the proton diffusion, thereby forming rich CO_2R three-phase interfaces for effective electroreduction of diluted CO_2 into C_{2+} products in strong acid. Our study provides a promising route to directly converting industrial flue gas into valuable products for energy- and carbon-efficient CO_2R technology.

Methods

Chemicals

Commercial copper nanoparticles (~100 nm), $Cu(NO_3)_2{\cdot}3H_2O$ (99%), $CuSO_4{\cdot}5H_2O$ (99%), KCl (99.5%), K_2SO_4 (99%), 1,3,5-benzenetricarboxylic acid (BTC, 98%), methanol (99.5%) and isopropanol (99.7%) were purchased from Shanghai Macklin Biochemical Technology Co. Ltd. High purity carbon dioxide gas (99.999%) and nitrogen gas (99.999%) were purchased from Praxair. Nafion 117 membrane was purchased from DuPont. All chemical reagents involved were used without further purification.

Preparation of Sustainion ionomer-coated GCE

The polyimide shadow mask containing circular micropatterns with diameters of 300 μm was fabricated through a direct laser engraving

(YLP-HC20, Han's Laser). Then the polyimide mask was attached on the surface of GCE and Sustainion ionomer (5 wt% in ethanol, XA-9, Dioxide Material) was sprayed onto it. After drying at 60 °C, the polyimide mask was peeled off to form the Sustainion ionomer micropatterns on the GCE.

Preparation of Sustainion ionomer-coated Cu

We used Cu-BTC as the Cu precursor, which was synthesized by mixing $Cu(NO)_3{\cdot}3H_2O$ (9.1 g) and BTC (0.79 g) in 250 mL methanol. The mixed solution was aged for 6 h at room temperature, followed by centrifugation and drying to obtain Cu-BTC. Then Cu-BTC was annealed at 350 °C for 3 h to obtain the CuO. Subsequently, 7 mg of CuO powder and 8 mg of Sustainion ionomer (5 wt% in ethanol) were dispersed via ultrasonication for 30 min to obtain a homogeneous catalyst ink, which was then sprayed onto a carbon paper-based GDE (YLS 30 T, Toray) with an area of 4 cm^2. Finally, Cu@Sustainion electrode was obtained through an electrochemical reduction process at a current density of -20 mA cm^{-2} for 30 min in 0.5 M K_2SO_4 electrolyte. The loading amounts of Cu and Sustainion ionomer are 1.4 and 0.1 mg cm^{-2}, respectively, corresponding to a mass fraction of 6.7 wt% for Sustainion ionomer. Cu@Sustainion electrodes with other Sustainion ionomer loadings of 0.05, 0.2, and 0.5 mg cm^{-2} were also prepared by adjusting the ionomer amounts.

For the preparation of Com-Cu@Sustainion, the process was similar with that for Cu@Sustainion except for replacing Cu with Com-Cu (Macklin). For the preparation of ED-Cu@Sustainion, the ED-Cu was first electrodeposited on GDE at -20 mA cm^{-2} for 10 min in 0.1 M $CuSO_4$ solution and then Sustainion ionomer was sprayed onto the GDE surface to obtain ED-Cu@Sustainion.

Characterization

SEM images were obtained from a scanning electron microscope (FEI Verios 460 L). TEM and HRTEM images were carried out on a transmission electron microscope (FEI Talos F200X). XRD patterns were recorded on an X-ray diffractometer (Japan Rigaku SmartLab 9 kW) with a Cu Kα radiation source (λ = 1.5418 Å). XPS spectra were collected on a Thermo Scientific ESCALAB250Xi spectrometer equipped with an Al Kα (hv = 1486.6 eV) excitation source. FTIR spectra were acquired by using a NICOLET FT-IR spectrometer. CO_2 bubble transport and water contact angle experiments were performed on a dynamic contact angle meter (SZ-CAMC33). CO_2 adhesive force measurements were carried out on a DataPhysics device (DCAT25). In situ ATR-SEIRAS spectra were collected by an FT-IR spectrometer (Nicolet iS50, Thermo Scientific) equipped with an MCT-A detector at different applied potentials.

CO_2R performance measurements and product analysis

We evaluated the CO_2R performance of catalysts in a three-electrode system in a flow cell. Catalyst-coated GDE, Ag/AgCl electrode, IrO_2-coated Pt/Ti mesh were used as the working electrode, reference electrode, and counter electrode, respectively. A strongly acidic solution containing 3.0 M KCl with 0.05 M H_2SO_4 (pH 0.8) was used as the electrolyte, and the electrolyte was used immediately after preparation without storage. The catholyte chamber was separated from the anolyte chamber by a proton exchange membrane (Nafion 117, 183 μm). The catholyte and anolyte were circulated by a peristaltic pump with a flow rate of 20 mL min^{-1}. The cathode was fed with pure CO_2 or diluted CO_2 (CO_2/N_2 = 15/85) controlled by a mass flow controller. In pure CO_2R electrolysis experiments, the gas flow rate is 25 sccm, and other flow rates were used for SPCE tests. In diluted CO_2R electrolysis experiments, the total gas flow rate is 50 sccm containing 15% CO_2, and other flow rates were used for SPCE tests.

The electrochemical results were recorded on an electrochemical workstation (AutoLab PGSTAT 302 N). The FEs of products were measured at a fixed current density. The stability was evaluated via a chronopotentiometry method at a current density of 500 mA cm^{-2}. The measured potentials versus Ag/AgCl electrode were converted to RHE scale with iR correction according to the following equation: E (vs. RHE) = E (vs. Ag/AgCl) + 0.196 V + 0.059 pH − iR, where R was 5 ± 0.3 Ω from the EIS test.

Gas-phase products were analyzed on an on-line gas chromatography system (Nexis GC-2030), and liquid-phase products were quantified on an NMR spectrometer (Bruker AVANCE III 400 MHz).

The FE of the products was calculated using the following method:

$$FE_{gas} = \frac{z \times F \times v \times r}{i \times V_m} \times 100\% \text{ and } FE_{liquid} = \frac{z \times F \times n}{Q} \times 100\%$$

Where z is the electron transfer number, F is Faraday's constant (96,485 C mol^{-1}), v is the gas flow rate measured at the reactor outlet (L min^{-1}), r is the detected gas product concentration in parts per million (ppm), i is the total applied current (A), V_m is the molar gas volume (24.5 L mol^{-1}), n is the moles of liquid products from NMR analysis (mol), and Q is the total charge (C).

The SPCE of CO_2R was calculated according to the following equation:

$$SPCE = \frac{60s \times \sum(i \times FE_i \times x_i \div (z \times F))}{y \times \text{flow rate}\,(L/\text{min}) \times 1\text{min}/24.5(L/\text{mol})}$$

where i is the total applied current (A), FE_i is the Faradaic efficiency for each CO_2R product, x_i is the molar ratio of CO_2 to each CO_2R product (such as $x = 1$ for C_1 product, $x = 2$ for C_2 product, and $x = 3$ for C_3 product), z is the electron transfer number for each CO_2R product, F is Faraday's constant, and y is volume fraction of CO_2 (such as $y = 100\%$ for pure CO_2 and $y = 15\%$ for diluted CO_2).

Data availability

The data that support the findings of this study are available within the paper and Supplementary Information files. Source data are provided with this paper.

References

1. Masel, R. I. et al. An industrial perspective on catalysts for low-temperature CO_2 electrolysis. *Nat. Nanotechnol.* **16**, 118–128 (2021).
2. Nitopi, S. et al. Progress and Perspectives of Electrochemical CO_2 Reduction on Copper in Aqueous Electrolyte. *Chem. Rev.* **119**, 7610–7672 (2019).
3. Kibria, M. G. et al. Electrochemical CO_2 reduction into chemical feedstocks: From mechanistic electrocatalysis models to system design. *Adv. Mater.* **31**, 1807166 (2019).
4. Wang, D. et al. Modulating microenvironments to enhance CO_2 electroreduction performance. *eScience* **3**, 100119 (2023).
5. Wakerley, D. et al. Gas diffusion electrodes, reactor designs and key metrics of low-temperature CO_2 electrolysers. *Nat. Energy* **7**, 130–143 (2022).
6. Yang, P.-P. & Gao, M.-R. Enrichment of reactants and intermediates for electrocatalytic CO_2 reduction. *Chem. Soc. Rev.* **52**, 4343–4380 (2023).
7. Kim, D. et al. Electrocatalytic reduction of low concentrations of CO_2 Gas in a membrane electrode assembly electrolyzer. *ACS Energy Lett.* **6**, 3488–3495 (2021).
8. Xu, Y. et al. Oxygen-tolerant electroproduction of C_2 products from simulated flue gas. *Energy Environ. Sci.* **13**, 554–561 (2020).
9. Cheng, Y., Hou, J. & Kang, P. Integrated capture and electroreduction of flue gas CO_2 to formate using amine functionalized SnO_x nanoparticles. *ACS Energy Lett.* **6**, 3352–3358 (2021).
10. Zhao, Z.-H. et al. Efficient capture and electroreduction of dilute CO_2 into highly pure and concentrated formic acid aqueous solution. *J. Am. Chem. Soc.* **146**, 14349–14356 (2024).

11. Jouny, M., Luc, W. & Jiao, F. General techno-economic analysis of CO_2 electrolysis systems. *Ind. Eng. Chem. Res.* **57**, 2165–2177 (2018).
12. Sullivan, I. et al. Coupling electrochemical CO_2 conversion with CO_2 capture. *Nat. Catal.* **4**, 952–958 (2021).
13. Hepburn, C. et al. The technological and economic prospects for CO_2 utilization and removal. *Nature* **575**, 87–97 (2019).
14. Kim, B. et al. Over a 15.9% Solar-to-CO conversion from dilute CO_2 streams catalyzed by gold nanoclusters exhibiting a high CO_2 binding affinity. *ACS Energy Lett.* **5**, 749–757 (2020).
15. Gao, D., Arán-Ais, R. M., Jeon, H. S. & Roldan Cuenya, B. Rational catalyst and electrolyte design for CO_2 electroreduction towards multicarbon products. *Nat. Catal.* **2**, 198–210 (2019).
16. Chang, B. et al. Electrochemical reduction of carbon dioxide to multicarbon (C_{2+}) products: challenges and perspectives. *Energy Environ. Sci.* **16**, 4714–4758 (2023).
17. Bushuyev, O. S. et al. What should we make with CO_2 and how can we make It? *Joule* **2**, 825–832 (2018).
18. Todorova, T. K., Schreiber, M. W. & Fontecave, M. Mechanistic understanding of CO_2 reduction reaction (CO_2RR) toward multicarbon products by heterogeneous copper-based catalysts. *ACS Catal.* **10**, 1754–1768 (2020).
19. García de Arquer, F. P. et al. CO_2 electrolysis to multicarbon products at activities greater than 1 A cm^{-2}. *Science* **367**, 661–666 (2020).
20. Wang, Y., Liu, J. & Zheng, G. Designing copper-based catalysts for efficient carbon dioxide electroreduction. *Adv. Mater.* **33**, 2005798 (2021).
21. Ma, Z. et al. CO_2 electroreduction to multicarbon products in strongly acidic electrolyte via synergistically modulating the local microenvironment. *Nat. Commun.* **13**, 7596 (2022).
22. Huang, J. E. et al. CO_2 electrolysis to multicarbon products in strong acid. *Science* **372**, 1074–1078 (2021).
23. Gu, J. et al. Modulating electric field distribution by alkali cations for CO_2 electroreduction in strongly acidic medium. *Nat. Catal.* **5**, 268–276 (2022).
24. Monteiro, M. C. O., Philips, M. F., Schouten, K. J. P. & Koper, M. T. M. Efficiency and selectivity of CO_2 reduction to CO on gold gas diffusion electrodes in acidic media. *Nat. Commun.* **12**, 4943 (2021).
25. Cao, Y. et al. Surface hydroxide promotes CO_2 electrolysis to ethylene in acidic conditions. *Nat. Commun.* **14**, 2387 (2023).
26. Wu, W. et al. Addressing the carbonate issue: Electrocatalysts for acidic CO_2 reduction reaction. *Adv. Mater.* **36**, 2312894 (2024).
27. Zeng, M. et al. Reaction environment regulation for electrocatalytic CO_2 reduction in acids. *Angew. Chem. Int. Ed.* **63**, e202404574 (2024).
28. Zhao, Y. et al. Conversion of CO_2 to multicarbon products in strong acid by controlling the catalyst microenvironment. *Nat. Synth.* **2**, 403–412 (2023).
29. Chen, Y. et al. Efficient multicarbon formation in acidic CO_2 reduction via tandem electrocatalysis. *Nat. Nanotechnol.* **19**, 311–318 (2024).
30. Zi, X. et al. Breaking K+ concentration limit on Cu nanoneedles for acidic electrocatalytic CO_2 reduction to multi-carbon products. *Angew. Chem. Int. Ed.* **62**, e202309351 (2023).
31. Xie, Y. et al. High carbon utilization in CO_2 reduction to multi-carbon products in acidic media. *Nat. Catal.* **5**, 564–570 (2022).
32. Nie, W., Heim, G. P., Watkins, N. B., Agapie, T. & Peters, J. C. Organic additive-derived films on Cu electrodes promote electrochemical CO_2 reduction to C_{2+} products under strongly acidic conditions. *Angew. Chem. Int. Ed.* **62**, e202216102 (2023).
33. Feng, J. et al. CO_2 electrolysis to multi-carbon products in strong acid at ampere-current levels on La-Cu spheres with channels. *Nat. Commun.* **15**, 4821 (2024).
34. Kim, C. et al. Tailored catalyst microenvironments for CO_2 electroreduction to multicarbon products on copper using bilayer ionomer coatings. *Nat. Energy* **6**, 1026–1034 (2021).
35. Sadeghpour, M., Yusoff, R. & Aroua, M. K. Polymeric ionic liquids (PILs) for CO_2 capture. *Rev. Chem. Eng.* **33**, 183–200 (2017).
36. Zhang, Q., Huang, Y. & Cao, R. Imidazolium-based materials for CO_2 electroreduction. *Acta Phys. Chim. Sin* **40**, 2306040 (2024).
37. Wang, S. & Wang, X. Imidazolium ionic liquids, imidazolylidene heterocyclic carbenes, and zeolitic imidazolate frameworks for CO_2 capture and photochemical reduction. *Angew. Chem. Int. Ed.* **55**, 2308–2320 (2016).
38. Kaczur, J. J., Yang, H., Liu, Z., Sajjad, S. D. & Masel, R. I. A review of the use of immobilized ionic liquids in the electrochemical conversion of CO_2. *C* **6**, 33 (2020).
39. Mukhopadhyay, S. et al. Local CO_2 reservoir layer promotes rapid and selective electrochemical CO_2 reduction. *Nat. Commun.* **15**, 3397 (2024).
40. Liu, Y., Ye, H.-Z., Diederichsen, K. M., Van Voorhis, T. & Hatton, T. A. Electrochemically mediated carbon dioxide separation with quinone chemistry in salt-concentrated aqueous media. *Nat. Commun.* **11**, 2278 (2020).
41. Simeon, F. et al. Electrochemical and molecular assessment of quinones as CO_2-binding redox molecules for carbon capture. *J. Phys. Chem. C* **126**, 1389–1399 (2022).
42. Sampson, M. D. et al. Manganese catalysts with bulky bipyridine ligands for the electrocatalytic reduction of carbon dioxide: eliminating dimerization and altering catalysis. *J. Am. Chem. Soc.* **136**, 5460–5471 (2014).
43. Ooka, H., Figueiredo, M. C. & Koper, M. T. M. Competition between hydrogen evolution and carbon dioxide reduction on copper electrodes in mildly acidic media. *Langmuir* **33**, 9307–9313 (2017).
44. Zhang, Q. et al. A covalent molecular design enabling efficient CO_2 reduction in strong acids. *Nat. Synth.* **3**, 1231–1242 (2024).
45. Wang, P. et al. Boosting electrocatalytic CO_2–to–ethanol production via asymmetric C–C coupling. *Nat. Commun.* **13**, 3754 (2022).
46. Chou, T.-C. et al. Controlling the oxidation state of the Cu electrode and reaction intermediates for electrochemical CO_2 reduction to ethylene. *J. Am. Chem. Soc.* **142**, 2857–2867 (2020).
47. Malkani, A. S., Dunwell, M. & Xu, B. Operando spectroscopic investigations of copper and oxide-derived copper catalysts for electrochemical CO reduction. *ACS Catal.* **9**, 474–478 (2019).
48. Pérez-Gallent, E., Figueiredo, M. C., Calle-Vallejo, F. & Koper, M. T. M. Spectroscopic observation of a hydrogenated CO dimer intermediate during CO reduction on Cu(100) electrodes. *Angew. Chem. Int. Ed.* **56**, 3621–3624 (2017).
49. Yao, K. et al. Mechanistic insights into OC–COH coupling in CO_2 electroreduction on fragmented copper. *J. Am. Chem. Soc.* **144**, 14005–14011 (2022).

Acknowledgements

This work was supported by National Key R&D Program of China (2022YFA1502902), and National Natural Science Foundation of China (21931007, 22375146, and 22109149).

Author contributions

Z.-Y.Y. and T.-B.L. conceived and designed the project. X.-R.Q. performed the experiments, collected and analyzed the data. J.-J.L., L.-L.W., H.L., Z.-T.Y., G.-J.F., X.-R.W., X.-X.C., and C.Z. provided the help to analyze the results. Z.-Y.Y. and T.-B.L. wrote and revised the manuscript.

Competing interests

The authors declare no competing interests.

Additional information

Supplementary information The online version contains supplementary material available at https://doi.org/10.1038/s41467-025-59783-2.

Correspondence and requests for materials should be addressed to Zi-You Yu or Tong-Bu Lu.

Peer review information *Nature Communications* thanks Wen-Bin Cai and the other, anonymous, reviewer(s) for their contribution to the peer review of this work. A peer review file is available.